

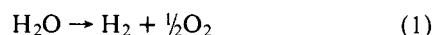
# Strontium Titanate Photoelectrodes. Efficient Photoassisted Electrolysis of Water at Zero Applied Potential

Mark S. Wrighton,\*<sup>1</sup> Arthur B. Ellis,<sup>2</sup> Peter T. Wolczanski, David L. Morse, Harmon B. Abrahamson, and David S. Ginley

Contribution from the Department of Chemistry, Massachusetts Institute of Technology, Cambridge, Massachusetts 02139. Received July 21, 1975

**Abstract:** Irradiation of an n-type semiconductor SrTiO<sub>3</sub> electrode in an electrochemical cell is shown to result in the sustained conversion of H<sub>2</sub>O to H<sub>2</sub> and O<sub>2</sub>. In 9.5 M NaOH oxidation occurs at the photoelectrode at potentials more positive than ca. -1.3 V vs. a saturated calomel electrode (SCE), and H<sub>2</sub> evolution is observed at the Pt electrode which is not illuminated. Results reported herein show for the first time that the electrolysis of H<sub>2</sub>O can be driven photochemically without any external bias. The photoeffect obtains upon irradiation with light of shorter wavelength than 390 nm which corresponds closely to the known absorption edge for the valence band to conduction band transition in SrTiO<sub>3</sub>. The photocurrent reaches its maximum value near 330 nm and the response is nearly constant with increasing excitation energy. Quantum efficiency for electron flow is found to be 1.0 ± 0.20 upon irradiation with light of shorter wavelength than 330 nm at applied potentials of ≥1.5 V. Current efficiency is excellent, producing H<sub>2</sub> and O<sub>2</sub> in the correct stoichiometric ratios. Photoelectrode stability has been confirmed by experiments carried out in oxygen-18 labeled H<sub>2</sub>O and by the lack of weight loss in the SrTiO<sub>3</sub>.

Sustained, photoinduced conversion of H<sub>2</sub>O to H<sub>2</sub> and O<sub>2</sub> using electrodes as photoassistance agents has recently been demonstrated using either Sb-doped SnO<sub>2</sub><sup>3</sup> or reduced TiO<sub>2</sub><sup>4</sup> as the photoelectrode. These n-type semiconductor electrodes of the rutile structure<sup>5</sup> are unique in that they do not undergo decomposition upon irradiation when used as a photoelectrode in aqueous media.<sup>6</sup> Photoeffects on semiconductor electrodes have been studied for some time,<sup>7</sup> and the initial results with TiO<sub>2</sub><sup>8</sup> have sparked considerable interest<sup>4,8-11</sup> in this material as a possible candidate for the photoelectrode in optical to chemical energy conversions using photoelectrochemical cells. In this report we present our results for a reduced SrTiO<sub>3</sub> photoelectrode which show that it will also serve as a photoelectrode for the electrolysis of H<sub>2</sub>O, reaction 1.

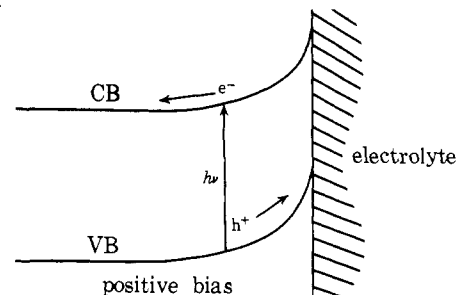


Like TiO<sub>2</sub> and SnO<sub>2</sub>, SrTiO<sub>3</sub> is extremely robust, and this reasoning alone led to our initial optimism concerning the prospects for its use as photoelectrode material. The SrTiO<sub>3</sub> has the simple cubic perovskite structure,<sup>12</sup> and when reduced is an n-type semiconductor.

Naturally, stability alone does not ensure that an electrode will be an optimum photoelectrode. Two other properties will define the efficiency of any electrode system used as a photoassistance agent in an optical to chemical energy conversion. One property of concern is the excitation wavelength necessary to run the reaction and the other is the energy required from an external power supply (other than the light). It is the hope of the investigators in this field that these three properties (stability, wavelength response, and current-voltage) can be manipulated to create an efficient device. Substantial photocurrent can be expected from a semiconductor photoelectrode by a valence band (VB) to conduction band (CB) transition, and typically onset of photoeffects corresponds to the absorption edge of the VB → CB transition. At standard conditions H<sub>2</sub>O can be reversibly electrolyzed at a potential of 1.23 V, but the sustained electrolysis may require ~1.5 V. Thus, an optimum photoelectrode would have a band gap (here taken to be equal to the VB → CB absorption edge) which is not smaller than 1.5 eV. However, a value substantially larger can "waste" light energy into heat.

With regard to applied potentials from an external power

Scheme I



supply in a photoelectrochemical cell (refer to Figure 1), net optical to chemical energy conversion obtains when the applied potential is less than 1.23 V. Ideally, a photoelectrochemical cell should operate with no external bias. For a semiconductor having a band gap larger than 1.5 eV the application of a potential is theoretically not necessary, but may be required to overcome cell impedances. Also, an applied potential may be required to achieve an effective *depletion region* at the surface of the electrode exposed to the electrolyte. It is known that a positive bias on an n-type semiconductor is favorable for the observation of photocurrents since the minority charge carriers, holes (h<sup>+</sup>), tend to go to the surface while the electrons (e<sup>-</sup>) go toward the bulk of the semiconductor, Scheme I.<sup>7</sup> Such inhibition of h<sup>+</sup>-e<sup>-</sup> recombination is seemingly a requirement in any efficient photoinduced electron transfer process which is endothermic. Neither TiO<sub>2</sub> (band gap ≈ 3.0)<sup>13</sup> nor SnO<sub>2</sub> (band gap ≈ 3.5)<sup>14</sup> has been shown to efficiently photoassist reaction 1 at zero bias. In this report we show that SrTiO<sub>3</sub> (band gap ≈ 3.2-3.4)<sup>15</sup> is nearly equivalent to TiO<sub>2</sub> and superior to SnO<sub>2</sub> with respect to wavelength response, and with respect to current-voltage properties SrTiO<sub>3</sub> is superior to either TiO<sub>2</sub> or SnO<sub>2</sub>. To our knowledge, this represents the first study of SrTiO<sub>3</sub> as the photoelectrode in an electrochemical cell.

## Results

**a. Apparatus and Electrodes.** All experiments have been carried out using a photoelectrochemical cell as shown in Figure 1. The Pt electrode has typically been a piece of Pt wire about 50 mm long and 1 mm in diameter. The variable applied potential source used was a Hewlett-Packard Model

## STANDARD PHOTOELECTROCHEMICAL CELL

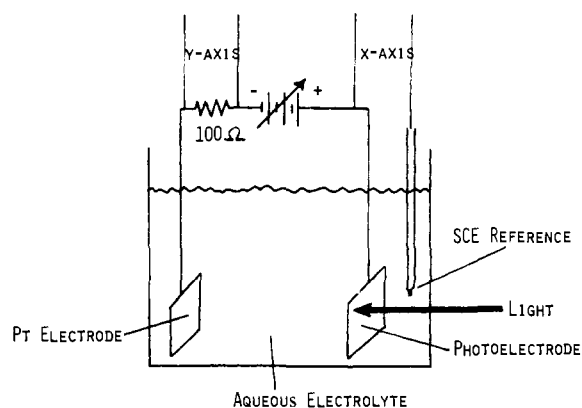


**Figure 1.** A typical photoelectrochemical cell. This is the type of cell used in the present work except that the SCE was often not present in the circuit.

6241A. Potential of the Pt or SrTiO<sub>3</sub> electrodes relative to the saturated calomel electrode (SCE) was monitored using a Hewlett-Packard Model 7044A x-y recorder and the current was measured by monitoring the potential drop across a resistor of a known value (typically 100 Ω) using either a Varian Model A-25 recorder or the x-y recorder. The irradiation source has been either a (1) Spectra Physics Model 164 argon ion laser tuned to the 351, 364 nm doublet emission or (2) a Bausch and Lomb mercury light source equipped with a 200-W Osram superhigh-pressure Hg arc lamp focused onto the photoelectrode. Quantum efficiency measurements were done using the laser source or the Bausch and Lomb source fitted with a monochromator. When the full output of the Bausch and Lomb source was used, 18 cm of H<sub>2</sub>O was employed to filter out near-ir irradiation to prevent excessive heating of the photoelectrode. In all cases where light intensities were measured ferrioxalate chemical actinometry<sup>16</sup> was used.

The SrTiO<sub>3</sub> was single-crystal material typically about 5 × 5 × 1 mm in dimensions for most experiments. A powder pattern confirmed its identity.<sup>17</sup> Semiconductivity of the SrTiO<sub>3</sub> was achieved by reduction with H<sub>2</sub> for 4 h at 1050–1100 °C. The resulting crystal is blue-black in appearance. A gallium–indium eutectic was rubbed onto the 5 × 5 surface of the SrTiO<sub>3</sub> and a copper wire was attached to this using conducting silver epoxy. The exposed metal was insulated by coating with a generous amount of ordinary epoxy. The electrode was encased in a glass tube in order to maintain its position in the cell. Data were collected using electrodes prepared from four different crystals of SrTiO<sub>3</sub> designated as A, B, C, and D.

Relative photocurrent as a function of incident wavelength has been determined by using the excitation optics of an Aminco-Bowman SPF-2 emission spectrometer equipped with a 150-W Xenon excitation lamp. The photoelectrochemical cell was simply positioned in the sample compartment of the Aminco such that the SrTiO<sub>3</sub> electrode was in the light beam. Correction of the response curve for variation in light intensity striking the electrode was accomplished by determining the relative light intensity at the sample in the 230–600-nm range using rhodamine B as a quantum counter.<sup>18</sup>

**b. Stoichiometry and Electrode Stability.** When the SrTiO<sub>3</sub> n-type semiconductor electrode in a cell as in Figure 1 is irradiated, current flows such that electrons flow from the SrTiO<sub>3</sub> towards the Pt electrode. In 9.5 M NaOH gas evolution at each electrode is very obvious when the applied potential (+ lead to SrTiO<sub>3</sub>) exceeds ~0.05 V (corresponding to an onset of photocurrent at an applied voltage

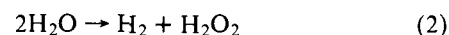
**Table I.** SrTiO<sub>3</sub> Electrode Stability<sup>a</sup>

Expt no.	Crystal	SrTiO <sub>3</sub> weight, g		Moles of SrTiO <sub>3</sub>		Moles of O <sub>2</sub> evolved
		Before	After	Before	After	
1	A	0.0599	0.0593	3.26 × 10 <sup>-4</sup>	3.23 × 10 <sup>-4</sup>	1.53 × 10 <sup>-4</sup>
2	B	0.1669	0.1635	9.26 × 10 <sup>-4</sup>	8.91 × 10 <sup>-4</sup>	5.99 × 10 <sup>-4</sup>
3	C	0.3097	0.3097	1.69 × 10 <sup>-3</sup>	1.69 × 10 <sup>-3</sup>	1.70 × 10 <sup>-4</sup>
4	D	0.3734	0.3739	2.04 × 10 <sup>-3</sup>	2.04 × 10 <sup>-3</sup>	1.55 × 10 <sup>-3</sup>

<sup>a</sup> These data were collected under variable conditions but at applied potentials of less than 3.0 V and where the stoichiometry was shown to correspond to the electrolysis of H<sub>2</sub>O.

of SrTiO<sub>3</sub> of –1.3 V vs. SCE, *vide infra*). We have observed absolute photocurrents of ~150 mA and current densities of over 200 mA/cm<sup>2</sup>. These currents, as far as we can tell, could be increased by increasing the light intensity. Using a cell without the SCE, purged with Ar, sealed, and fitted with gas collection chambers over both Pt and SrTiO<sub>3</sub>, we have been able to determine the identity of the gases by mass spectroscopy with a Hitachi-Perkin-Elmer RMU-6 mass spectrometer. With 9.5 M NaOH in H<sub>2</sub><sup>18</sup>O/H<sub>2</sub>O (1/4 by volume) as solvent, H<sub>2</sub> is evolved at the Pt electrode and a mixture of isotopes of O<sub>2</sub> are evolved at the SrTiO<sub>3</sub>. The statistical ratio of gases expected is <sup>16</sup>O<sub>2</sub> (100), <sup>16</sup>O<sup>18</sup>O (40.4), and <sup>18</sup>O<sub>2</sub> (2.4), and we found <sup>16</sup>O<sub>2</sub> (100), <sup>16</sup>O<sup>18</sup>O (36.6), and <sup>18</sup>O<sub>2</sub> (3.8). The oxygen-18 labeling experiment confirms that H<sub>2</sub>O is being oxidized and the O<sub>2</sub> evolved is not coming from decomposition of the SrTiO<sub>3</sub>. Electrode stability was confirmed directly by measuring weight loss of a SrTiO<sub>3</sub> crystal for situations where the amount of O<sub>2</sub> evolved is of the same order of magnitude as the amount potentially available from the semiconductor. The results are shown in Table I. Actually, the resiliency of the SrTiO<sub>3</sub> is much larger than that reflected by the data in Table I. The weight loss in the crystal is likely due to the partial loss of material when the SrTiO<sub>3</sub> crystal is recovered from the electrode and the gallium–indium eutectic and epoxy are scraped from the surface. No SrTiO<sub>3</sub> photoelectrode has ceased operating due to decomposition of the SrTiO<sub>3</sub>. The major problems associated with maintaining a constant photocurrent for a long period are (1) variations in excitation source intensity, and (2) deterioration of the epoxy insulation followed by chemical attack on the silver epoxy, gallium–indium eutectic, or copper wire. *By all reasonable measures, the SrTiO<sub>3</sub> is indestructible under conditions where the electrolysis of H<sub>2</sub>O can be photoassisted.*

Data in Table II show several sets of stoichiometric measurements for integrated current, H<sub>2</sub> production, and O<sub>2</sub> production. In strongly alkaline solutions the ratio of moles of electrons to moles of H<sub>2</sub> to moles of O<sub>2</sub> is very nearly 4:2:1 as expected for the electrolysis of H<sub>2</sub>O, reaction 1. In less alkaline media the electrons to H<sub>2</sub> balance remains close to 2:1, but the amount of O<sub>2</sub> found is less than expected. We suspect that the deficiency of O<sub>2</sub> can be accounted for, at least in part, by the formation of H<sub>2</sub>O<sub>2</sub>. That is, reaction 2 may obtain to some extent. Evidence for H<sub>2</sub>O<sub>2</sub> production has been obtained in acidic solutions where H<sub>2</sub>O<sub>2</sub> is



relatively stable. The H<sub>2</sub>O<sub>2</sub> was detected by an iodometric titration<sup>19</sup> and was found to account for a substantial fraction of the O<sub>2</sub> deficiency. In more basic solutions H<sub>2</sub>O<sub>2</sub> does decompose into O<sub>2</sub> and H<sub>2</sub>O but we would not have collect-

Table II. Stoichiometry of SrTiO<sub>3</sub> Photoassisted Electrolysis of H<sub>2</sub>O

Crystal <sup>a</sup>	Electrolyte	Applied <sup>b</sup> potential, V	Av current, <sup>c</sup> mA	Irrdn <sup>d</sup> time, h	Moles × 10 <sup>4</sup>		
					Electrons	H <sub>2</sub>	O <sub>2</sub>
A	9.5 M NaOH	1.0	0.60	21.1	5.8	3.1	1.5
B	9.1 M NaOH	2.8	3.36	1.24	1.6	0.90	0.43
B	9.1 M NaOH	1.3	1.50	6.12	3.4	1.6	0.78
B	9.1 M NaOH	0.0	0.37	10.2	1.4	0.78	0.35
B	0.07 M NaOH	2.8	4.53	3.60	6.1	2.9	1.1
B	1.0 M HClO <sub>4</sub>	1.0	1.0	5.75	2.1	1.1	0.37
C	9.1 M NaOH	1.0	3.60	3.00	4.0	2.1	0.92
C	9.1 M NaOH	0.0	0.13	65.0	3.2	1.7	0.78
D	9.1 M NaOH	0.5	19.2	8.4	60	32	16

<sup>a</sup> Cf. Table I for weights of these crystals of SrTiO<sub>3</sub>. <sup>b</sup> Positive lead to SrTiO<sub>3</sub>. <sup>c</sup> Determined by measuring potential drop across a 100-Ω resistor in series. <sup>d</sup> Irradiation source is the full output (H<sub>2</sub>O filtered) of the super-pressure 200-W Hg lamp focused on the photoelectrode.

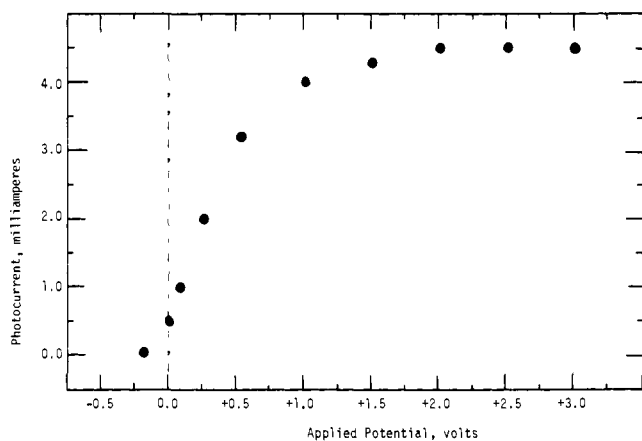


Figure 2. Photocurrent vs. applied potential (+ lead to SrTiO<sub>3</sub>) for crystal B (Table I) in 9.5 M NaOH. Light source is the 200-W superhigh-pressure Hg lamp. The power supply is simply in series in the external circuit.

ed the O<sub>2</sub> under the conditions of our experiments, since we collect the O<sub>2</sub> and H<sub>2</sub> in 10-ml graduated cylinders immediately above the electrodes. In all cases, though, the stoichiometry is fairly close to the expected, and at this point there is every indication that the SrTiO<sub>3</sub> does serve as a photoassistance agent for the electrolysis of H<sub>2</sub>O.

**c. Current-Voltage Properties.** First, the photocurrent as a function of applied potential has been measured in 9.5 M NaOH, Figure 2. As the applied potential (+ lead to SrTiO<sub>3</sub>) is increased, the observed photocurrent increases rapidly, and at potentials exceeding ~2.0 V there is a constant photocurrent. The points to note here are: (1) there is a reasonable photocurrent (~10% of the maximum) at zero applied potential; (2) there is a sharp increase in the photocurrent with increasing applied potential, at 0.25 V ~50% photoeffect obtains; (3) there is no increase in photocurrent above 2.0 V. A perfect electrode system would show the onset of a dark electrolytic decomposition of H<sub>2</sub>O at 1.23 V; thus, the effect of light phenomenologically has been to reduce the required decomposition voltage to zero or less, but the *maximum* photocurrent still does not obtain at zero applied potential. However, the results here for SrTiO<sub>3</sub> are substantially better than those reported for TiO<sub>2</sub><sup>8</sup> or SnO<sub>2</sub>.<sup>3</sup> The current-voltage curve for SrTiO<sub>3</sub> (crystal B of Table I) vs. SCE is shown in Figure 3 and shows an onset of photoeffect near -1.3 V in 9.5 M NaOH. The current-voltage curve is independent of the excitation wavelength. *The current-voltage data given in Figures 2 and 3 show that the onset of photocurrent for SrTiO<sub>3</sub> is at more negative potentials and the photocurrent increases more sharply with*

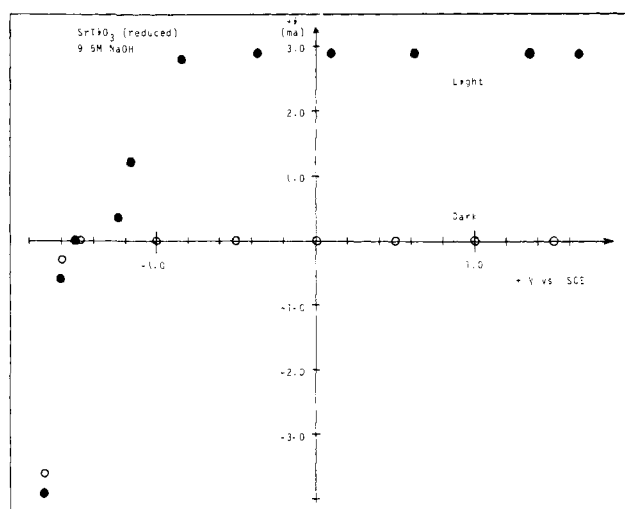


Figure 3. Current-voltage curve for SrTiO<sub>3</sub> (crystal B). Potential of SrTiO<sub>3</sub> photoelectrode is shown relative to the SCE. The solution is 9.5 M NaOH.

*increasing applied potential than for either the TiO<sub>2</sub> or SnO<sub>2</sub>.<sup>20</sup>*

We have had some difficulty in obtaining the now reproducible data shown in Figures 2 and 3 and have traced the problems, we feel, to instability of the SCE in 9.5 M NaOH and to the manner in which the contact to the SrTiO<sub>3</sub> crystal is made. The first data were recorded using a SrTiO<sub>3</sub> electrode where the contact was made using the gallium-indium eutectic and then attaching the copper wire using the silver epoxy. The electrode was then demounted and when reassembled the copper wire was attached with only the silver epoxy. Without the gallium-indium eutectic backing, substantially higher potentials (~400 mV) were required to make the electrode give the same photocurrents as previously obtained. Demounting the crystal and putting the gallium-indium backing on the crystal regenerated the optimum current-voltage properties shown in Figures 2 and 3. At optimum conditions crystals C and D have current-voltage curves similar to those given for crystal B. The point of emphasis here is that cell impedances should be minimized to achieve optimum current-voltage curves. The resistances of the electrodes exhibiting optimum current-voltage properties have been determined to be quite small, ≤5 Ω. The determination was made by first establishing a second good contact to the electrode by rubbing the gallium-indium eutectic onto the surface of the SrTiO<sub>3</sub> typically exposed to the electrolyte. The resistance was then measured using a Simpson meter by attaching one probe to the copper

**Table III.** Light Intensity Effect on Maximum Photocurrent<sup>a</sup>

Rel light intens	Neutral <sup>b</sup> density screens, OD	Max photocurrent, mA
1413	None	17.4
79.4	1.25	1.12
17.8	1.90	0.278
1.0	1.25 + 1.90 <sup>c</sup>	0.017

<sup>a</sup> Maximum photocurrent recorded in 9.5 M NaOH at an applied potential of 2.0 V (+ lead to SrTiO<sub>3</sub>). <sup>b</sup> Neutral density screens having the indicated optical density were placed in the light beam to vary the intensity striking the electrode. <sup>c</sup> Two screens placed ~2.5 cm apart in the light beam.

lead of the electrode and touching the other probe to the gallium-indium contact.

At low light intensities the impedance to current flow rests mainly in the fact that holes are not produced at a sufficiently fast rate to allow a substantial current to flow. At the high light intensity extreme, impedances to current flow are just those associated with any conventional electrochemical cell, and variations in the circuit resistances would be manifested as variations in the slope of the current-voltage curve in the region where the photocurrent increases approximately linearly with increasing applied potential. Since the 100- $\Omega$  resistor used to measure the current may be a significant resistance in the circuit, we determined a decomposition current-voltage curve using a 5-, 15-, 100-, and 8200- $\Omega$  dropping resistor at a light intensity such that the maximum photocurrent was ~5 mA. The 5- and 15- $\Omega$  resistors gave similar curves but each yielded a more steeply rising photocurrent than the 100- $\Omega$  resistor. For example, at 0.25 V applied the photocurrent with a 100- $\Omega$  resistor was 44% of the maximum, while with the 15- $\Omega$  resistor the 0.25 V applied yielded a photocurrent of 67% of the maximum. As expected, the 8200- $\Omega$  resistor was found to be a severe impedance to current flow. At potentials where polarization of the photoelectrode is complete it is expected that the current will depend only on the light intensity. We find the same relative photocurrent for the 5-, 15-, and 100- $\Omega$  dropping resistors above the potential where the electrode polarization is complete, and additionally, the maximum photocurrent with a 15- $\Omega$  dropping resistor varied nearly linearly with a 1000-fold change in light intensity, Table III.

One point should be made firmly. The current-voltage curves show that a sizable photocurrent obtains at zero applied potential. The electrode processes corresponding to this current flow are the same as those occurring at the potentials where the maximum photoeffect obtains. This conclusion is unequivocally established by data in Table II that show that the stoichiometry at zero applied potential corresponds to the electrolysis of H<sub>2</sub>O. Thus, the SrTiO<sub>3</sub> photoelectrode is demonstrated to sustain the photoinduced conversion of H<sub>2</sub>O to H<sub>2</sub> and O<sub>2</sub> without the need of an external bias. The stoichiometric determination is required since it has been shown that photocurrents found at zero applied potential for TiO<sub>2</sub> may correspond to the reduction of dissolved O<sub>2</sub><sup>9,10</sup> or other impurities<sup>4</sup> and not the reduction of H<sub>2</sub>O.

**d. Wavelength Response and Quantum Efficiency.** The band gap of SrTiO<sub>3</sub> corresponds reasonably well to the onset of photocurrent that we find, Figure 4. The photocurrent for SrTiO<sub>3</sub> increases in the near-uv and levels off above ~330 nm. Like TiO<sub>2</sub><sup>4</sup> and SnO<sub>2</sub>,<sup>3</sup> SrTiO<sub>3</sub> photoelectrodes, then, do not efficiently use the solar irradiation. Moreover, the threshold of 400 nm far exceeds the minimum energy required for the photoelectrolysis of H<sub>2</sub>O. Photoresponse of the SrTiO<sub>3</sub>, though, is at substantially lower energy than

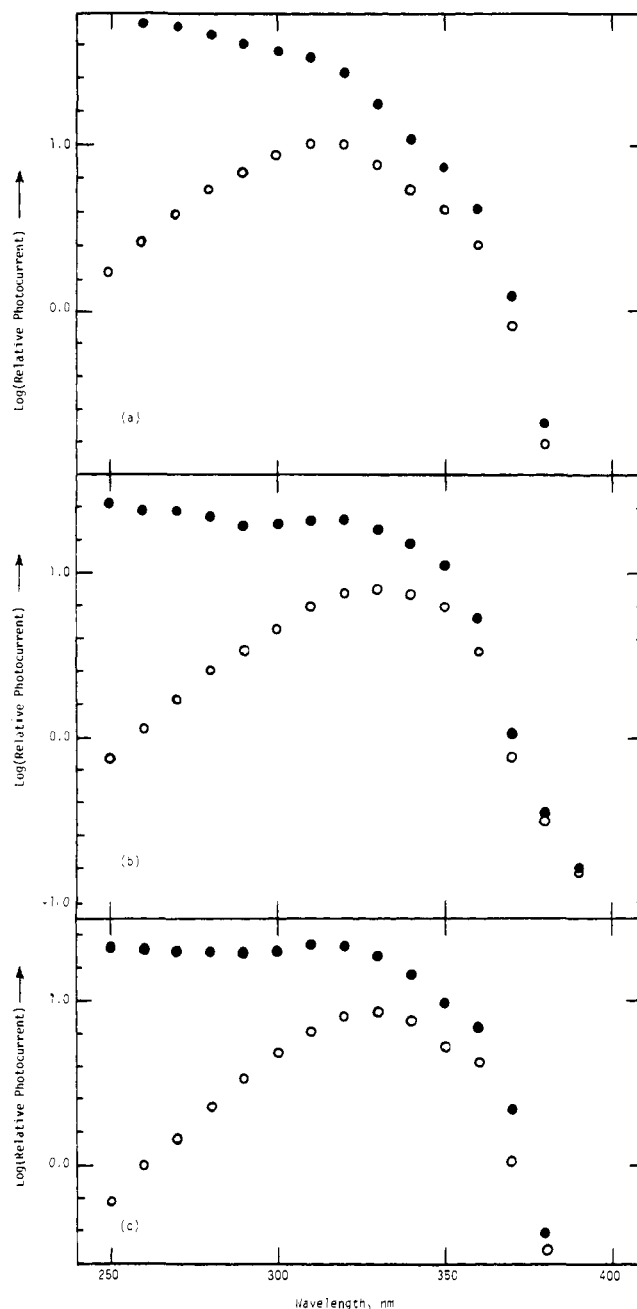


**Figure 4.** Relative photocurrent as a function of the wavelength of the incident light for SrTiO<sub>3</sub> crystal D (a), C (b), and B (c). Data points are taken every 10 nm and (O) are observed response and (●) are values corrected for variation in incident light intensity with wavelength.

SnO<sub>2</sub> and compares well with TiO<sub>2</sub>. It is interesting to note that while the essential wavelength dependence of the three SrTiO<sub>3</sub> crystals is invariant, there are some minor differences in the curves shown in Figure 4. We do not understand the source of these fluctuations in wavelength properties.

In view of the apparent changes in the stoichiometry with variation in NaOH concentration (Table II), we examined the relative quantum efficiency for electron flow as a function of NaOH concentration. We simply measured the photocurrent at an applied potential where the maximum photoeffect obtains in all cases. Data are given in Table IV that show in the range 0.025–9.1 M NaOH the maximum quantum efficiency is constant. Indeed, even the decomposition current-voltage curves are quite similar for all concentrations studied. Only with the 0.025 M NaOH solution did we

**Table IV.** Relative SrTiO<sub>3</sub> Photocurrent as a Function of NaOH Concentration<sup>a</sup>

Reading no.	NaOH, M	Photocurrent, mA ± 0.2
1	0.91	2.65
2	4.55	2.75
3	9.10	2.40
4	0.18	2.75
5	9.10	2.30
6	0.025	2.30

<sup>a</sup> Experiment carried out with a Pt-wire dark electrode and crystal B of Table I as the photoelectrode. An applied potential of 2.8 V (+ lead to SrTiO<sub>3</sub>) was used to ensure that maximum photoeffect obtained for each solution. Conditions are exactly the same for each reading except for NaOH concentration. Photocurrent was recorded after 30 min of equilibration, and the reading no. is given in the sequence actually recorded.

**Table V.** Quantum Efficiency for Electron Flow for SrTiO<sub>3</sub> Photoelectrodes

Crystal	Wavelength, nm	Intensity (einstein/min)	Φ ± 20% <sup>a</sup>
B	351, 364 <sup>b</sup>	4.47 × 10 <sup>-6</sup>	0.11
		2.92 × 10 <sup>-6</sup>	0.13
		8.16 × 10 <sup>-7</sup>	0.11
C	351, 364 <sup>b</sup>	1.83 × 10 <sup>-6</sup>	0.18
		1.35 × 10 <sup>-7</sup>	1.05
		254 <sup>c</sup>	1.13 × 10 <sup>-7</sup>
D	313 <sup>c</sup>	1.35 × 10 <sup>-7</sup>	1.15
		254 <sup>c</sup>	1.13 × 10 <sup>-7</sup>

<sup>a</sup> All data are at 25 °C in 9.5 M NaOH solutions. The current was determined by measuring the potential drop across a 100-Ω resistor in series in the circuit. The applied potential is that necessary to achieve the maximum photocurrent (1.5–2.0 V); cf. Figure 2. <sup>b</sup> Doublet emission from argon ion laser. <sup>c</sup> Bausch and Lomb source with monochromator.

note that the photocurrent rises less steeply with increasing applied potential than the more concentrated solutions. The measurable difference in current-voltage properties is likely a logical consequence of increasing the cell resistance by decreasing the ion concentration in the solution. Also, the flat-band potential of the photoelectrode is a function of pH and ion concentration which may result in alteration of the current-voltage curves.

Absolute quantum efficiency for electron flow has been measured with three different crystals and three different excitation energies. Data are summarized in Table V for the several determinations that we have made. As reflected by the quantum yield data and the data given in Figure 4, every photon of wavelength shorter than 330 nm incident on the SrTiO<sub>3</sub> photoelectrode produces an electron in the external circuit, when the applied potential is ≥ 1.5 V. While we feel that every photon *absorbed* corresponding to a VB to CB transition results in one electron when the applied potential exceeds ~1.5 V, the light of wavelength longer than ~330 nm is not absorbed totally efficiently within the depletion region resulting in *observed* quantum efficiencies of less than unity in the 390–330-nm range. Thus, for excitations at or above 330 nm in energy the quantum efficiency for H<sub>2</sub> formation is at the theoretical limit of 0.5 at applied potentials exceeding 1.5 V. At lower applied potentials the quantum efficiency can be determined from the current-voltage curves like that shown in Figure 2. For example, at 0.25 V applied, the photoeffect is ~50% of the maximum and the quantum efficiency for H<sub>2</sub> formation is therefore only 0.25.

## Discussion

In the Results section we have included some considerable discussion of the differences between SnO<sub>2</sub>, TiO<sub>2</sub>, and SrTiO<sub>3</sub> photoelectrodes. We now wish to discuss the optical energy conversion efficiency of the SrTiO<sub>3</sub> system. It should be emphasized at the outset that the SrTiO<sub>3</sub> photoelectrode system is not an efficient device for the conversion of unperturbed, terrestrial, *solar* energy to chemical energy. This statement follows from the well known fact that only ~3% of the solar energy comes from light of shorter wavelength than 400 nm.<sup>21</sup> Thus, the wavelength response of the SrTiO<sub>3</sub> photoelectrode limits its utility as an efficient solar energy device. However, the discussion below will show that the SrTiO<sub>3</sub> photoelectrode system is an impressively efficient *photochemical* storage system for ultraviolet light.

The overall efficiency of the energy conversion by the photoassisted electrolysis of H<sub>2</sub>O is governed by the quantum efficiency, the energy of the excitation light, the applied potential required, the current efficiency, and the *recoverable* energy from the photogenerated fuel. The data in Table II support the contention that the current efficiency is essentially 100%, and we will assume for the remaining discussion that the current efficiency is 100%. Observed quantum efficiency is wavelength dependent, Figure 4, but the increase from the onset at 390 nm to the maximum efficiency at ~330 nm is quite sharp, and, consequently, we will make estimations of the maximum optical conversion efficiency assuming incident light of 330 nm. We will assume that the maximum recoverable energy from H<sub>2</sub> and ½O<sub>2</sub> is the standard free energy of formation of liquid H<sub>2</sub>O, 56.7 kcal/mol.<sup>22</sup> The maximum optical conversion efficiency, η<sub>max</sub>, will depend on applied potential since the quantum efficiency is dependent on the applied potential. We choose to define the optical energy conversion efficiency, η, as indicated in eq 3.

$$\eta = \frac{[\text{energy stored as H}_2] \sim [\text{energy in from power supply}]}{[\text{energy in from light}]} \quad (3)$$

The value of η can be calculated from data given in the results using eq 4 and the quantum efficiency for electron flow, Φ; the applied potential from the power supply, V<sub>appl</sub>; the energy from the light, 330 nm = 86.7 kcal/einstein; and the energy from the H<sub>2</sub> = 56.7 kcal/mol.

$$\eta = \frac{[\Phi][(0.5)(56.7) - (23.07)(V_{\text{appl}})]}{[86.7]} \quad (4)$$

The factor of 0.5 is introduced to account for the fact that two electrons flow per molecule of H<sub>2</sub>, and 23.07 is the conversion factor to change volts to kilocalories/mole.

Obviously, when the applied potential from the power supply exceeds ~1.23 V the efficiency of the storage of optical energy is not positive. Using a current-voltage curve like that shown in Figure 2 reveals that the η<sub>max</sub> occurs at an applied potential between 0.25 and 0.40 V. The largest value of η<sub>max</sub> that we have observed is ~0.20. This represents an exceptional increase over the ~0.02 η<sub>max</sub> that we obtained from the TiO<sub>2</sub><sup>4</sup> using the same definition for optical storage efficiency. Conversion of light energy to useful chemical energy with the 20% efficiency reported here is an especially noteworthy achievement since the product (H<sub>2</sub>) is actually a useful form of chemical energy.

If we consider the total energy conversion efficiency (electrical + optical), T<sub>η</sub>, as defined in eq 5, we have obtained values of T<sub>η</sub> as high as 0.26.

$$T_{\eta} = \frac{[\Phi][(0.5)(56.7)]}{[(86.7) + (\Phi)(23.07)(V_{\text{appl}})]} \quad (5)$$

Thus, the total energy input is fairly efficiently converted to a useful chemical energy source in the form of H<sub>2</sub>. These considerations merely show that electrode photoassistance agents do provide viable mechanisms for storage of optical energy. It is wholly inappropriate at the present time to make detailed, rigorous comparisons of TiO<sub>2</sub>, SnO<sub>2</sub>, and SrTiO<sub>3</sub>, since the ultimate efficiencies are likely to be a sensitive function of electrode preparation and cell design. Nonetheless, the SrTiO<sub>3</sub> does have the best demonstrated efficiency.

The high energy conversion efficiencies claimed here are, in part, a consequence of the very small bias required from an external power supply. We are currently undertaking detailed studies of the photoelectrodes in order to probe the properties which influence the current-voltage characteristics. While the usefulness with regard to solar energy will remain minimal unless wavelength response is substantially red-shifted, the optical to chemical energy conversion efficiency can be improved for SrTiO<sub>3</sub> by simply attempting to photoassist a more endothermic reaction than the electrolysis of H<sub>2</sub>O.

**Note Added in Proof:** Findings similar to those reported here have just appeared in a preliminary communication: J. G. Mavroides, J. A. Kafalas, and D. F. Kolesar, *Appl. Phys. Lett.*, **28**, 241 (1976).

**Acknowledgment.** We thank the National Aeronautics and Space Administration for support of this research. We acknowledge useful discussions with Drs. A. Linz and David Epstein.

#### References and Notes

- (1) Fellow of the Alfred P. Sloan Foundation, 1974-1976.
- (2) Fannie and John Hertz Foundation Fellow.

- (3) M. S. Wrighton, D. L. Morse, A. B. Ellis, D. S. Ginley, and H. B. Abrahamson, *J. Am. Chem. Soc.*, **98**, 44 (1976).
- (4) M. S. Wrighton, D. S. Ginley, P. T. Wolczanski, A. B. Ellis, D. L. Morse, and A. Linz, *Proc. Natl. Acad. Sci. U.S.A.*, **72**, 1518 (1975).
- (5) R. W. G. Wyckoff, "Crystal Structures", 2nd ed, Vol. 1, Wiley, New York, N.Y., 1963.
- (6) For a discussion of semiconductor photoelectrode decomposition cf. H. Gerischer and W. Mindt, *Electrochim. Acta*, **13**, 1239 (1968).
- (7) For reviews cf. (a) T. Freund and W. P. Gomes, *Catal. Rev.*, **3**, 1 (1969); (b) V. A. Myamiin and Yu. V. Pleskov, "Electrochemistry of Semiconductors", Plenum Press, New York, N.Y., 1967; (c) H. Gerischer in "Physical Chemistry", Vol. IXA, H. Eyring, D. Henderson, and W. Jost, Ed., Academic Press, New York, N.Y., 1970, Chapter 5.
- (8) A. Fujishima and K. Honda, *Nature (London)*, **238**, 37 (1972), and *Bull. Chem. Soc. Jpn.*, **44**, 1148 (1971).
- (9) J. Keeney, D. H. Weinstein, and G. M. Haas, *Nature (London)*, **253**, 719 (1975).
- (10) W. Gissler, P. L. Lensi, and S. Pizzini, *J. Appl. Electrochem.*, **6**, 9 (1976).
- (11) (a) K. L. Hardee and A. J. Bard, *J. Electrochem. Soc.*, **122**, 739 (1975); (b) F. Mollers, J. J. Tolle, and R. Memming, *ibid.*, **121**, 1160 (1974); (c) H. Yoneyama, H. Sakamoto, and H. Tamura, *Electrochim. Acta*, **20**, 341 (1975); (d) A. J. Nozik, *Nature (London)*, **257**, 383 (1975); (e) T. Ohnishi, Y. Nakato, and H. Tsubomura, *Ber. Bunsenges. Phys. Chem.*, **79**, 523 (1975); (f) A. Fujishima, K. Kohayakawa, and K. Honda, *Bull. Chem. Soc. Jpn.*, **48**, 1041 (1975).
- (12) A. H. Kahn and A. J. Leyendeker, *Phys. Rev. [Sect.] A*, **135**, 1312 (1964).
- (13) D. C. Cronemeyer, *Phys. Rev.*, **87**, 876 (1972).
- (14) M. Nagasawa and S. Shionoya, *J. Phys. Soc. Jpn.*, **30**, 1118 (1971).
- (15) (a) T. A. Noland, *Phys. Rev.*, **94**, 724 (1954); (b) M. Cardona, *ibid.*, **140**, A 651 (1965); (c) M. I. Cohen and R. F. Blunt, *ibid.*, **168**, 929 (1968).
- (16) C. H. Hatchard and C. A. Parker, *Proc. R. Soc. London, Ser. A*, **235**, 518 (1956).
- (17) "Powder Diffraction File", Inorganic Vol., No. PD1S-5IRB, Set 5-0634, Joint Committee on Powder Diffraction Standards, Philadelphia, Pa., 1960.
- (18) W. H. Melhuus, *J. Opt. Soc. Am.*, **52**, 1256 (1962).
- (19) I. M. Kolthoff and E. B. Sandell, "Textbook of Quantitative Inorganic Analyses", 3rd ed, Macmillan, New York, N.Y., 1952, p 600.
- (20) We have determined the current-voltage properties of SnO<sub>2</sub> and TiO<sub>2</sub> in 9.5 M NaOH and have never obtained properties as good as those reported here for SrTiO<sub>3</sub>. It is clear, however, that such properties will be a significant function of electrode material and its treatment in preparation.
- (21) M. D. Archer, *J. Appl. Electrochem.*, **5**, 17 (1975).
- (22) W. J. Moore, "Physical Chemistry", 3rd ed, Prentice-Hall, Englewood Cliffs, N.J., 1962, p 172.

## A Calorimetric and <sup>1</sup>H Nuclear Magnetic Resonance Investigation of the Reaction of Triphenyl Phosphite with Compounds of the Type *trans*-Dichloro(pyridine)(olefin)platinum(II)

Walter Partenheimer

Contribution from the Department of Chemistry, Clarkson College of Technology, Potsdam, New York 13676. Received November 18, 1974

**Abstract:** The characterization and calorimetric results are reported for the following reactions: [PtCl<sub>2</sub>(olefin)]<sub>2</sub> + 2py → 2[PtCl<sub>2</sub>py(olefin)] (1); [PtCl<sub>2</sub>py(olefin)] + P(OC<sub>6</sub>H<sub>5</sub>)<sub>3</sub> → [PtCl<sub>2</sub>py(P(OC<sub>6</sub>H<sub>5</sub>)<sub>3</sub>)] + olefin (2); [PtCl<sub>2</sub>py(P(OC<sub>6</sub>H<sub>5</sub>)<sub>3</sub>)] + P(OC<sub>6</sub>H<sub>5</sub>)<sub>3</sub> → [PtCl<sub>2</sub>(P(OC<sub>6</sub>H<sub>5</sub>)<sub>3</sub>)<sub>2</sub>] + py (3). The enthalpies of the reactions are, within 6%, the same in benzene and dichloromethane and the relative displacement energies are triphenyl phosphite ≫ ethylene > cyclooctene > *cis*-butene > styrene > cyclopentene > nitrostyrene > cyclohexene. The displacement energies of Ag(I), Pd(II), Rh(I), Pt(II), and Ni(0) are compared and discussed. The coordination chemical shift of the olefin increases and the platinum-coupling decreases as the metal-olefin interaction increases. All three reactions proceed to completion when equimolar amounts of reactants are added, and reaction 3 has a rate constant of 8.9 ± 0.6 and reactions 1 and 2 have rate constants > 80 l. s<sup>-1</sup> mol<sup>-1</sup>. A thermodynamic description of the *trans* effect is given.

We have been interested in obtaining enthalpic and kinetic data on the formation and displacement of olefins with metals which may provide insight into the variety of catalytic processes which involve metal-olefin compounds. Initial studies involved common chelating polyolefins coordi-

nated to palladium(II)<sup>1</sup> and rhodium(I),<sup>2</sup> with subsequent studies on silver(I)<sup>3</sup> and palladium(II)<sup>4</sup> monoolefin compounds. Platinum(II) olefin compounds have a long history, are exceptionally stable, and have been studied extensively by a variety of physical techniques. We were therefore very